Biopolymers

Peptide Science

VOLUME 102, NUMBER 6, 2014

THE AMERICAN PEPTIDE SOCIETY JOURNAL

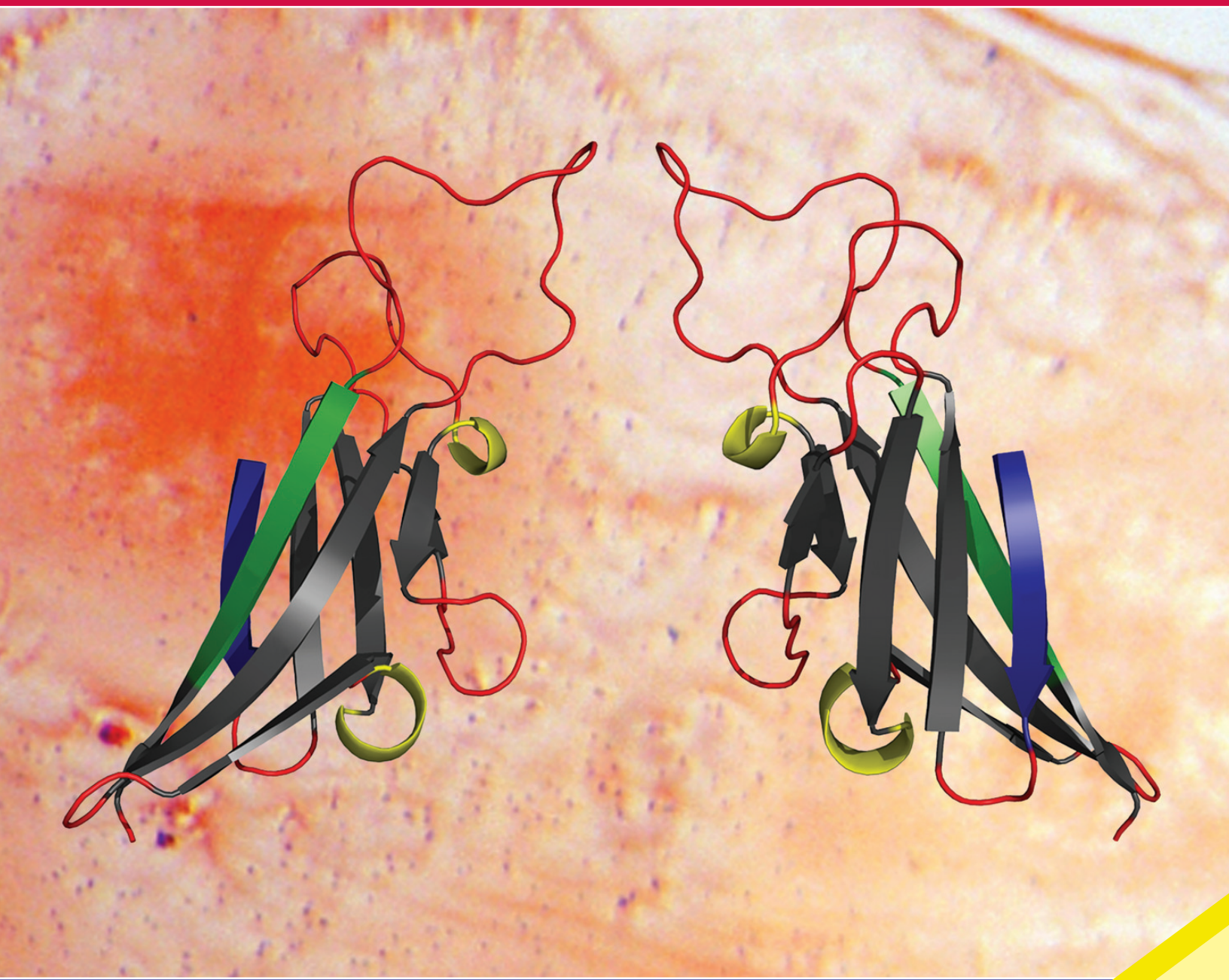

VIEW THIS JOURNAL ONLINE AT WILEYONLINELIBRARY.COM

WILEY Blackwell

Table of Contents

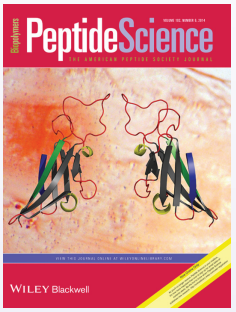

Cover Illustration: A model of teleostean ZPB ZP-N consensus sequence superimposed on a gel formed from one its derive peptides. A contribution from the Hamodrakas laboratory, University of Athens, Greece.

Biopolymers and Peptide Science are now publishing Preprints online within 5 days of acceptance*! Preprints are peer-reviewed articles that are published online in *EarlyView*® before copyediting and author correction. Preprint articles are citable by DOI. The final copyedited, author-corrected, paginated version is available shortly thereafter—within 12 weeks of first submission.

*Upon receipt of all necessary materials (figure files, signed Copyright Transfer Agreement, etc. from authors).

Editorial

Articles

Structural Studies of "Aggregation-prone" Peptide-analogues of Teleostean Egg Chorion ZPB Proteins

Nikolaos N. Louros,[1] Nektaria Petronikolou,[1] Theodoros Karamanos,[1] Paul Cordopatis,[2] Vassiliki A. Iconomidou,[1] Stavros J. Hamodrakas[1]

[1]*Department of Cell Biology and Biophysics, Faculty of Biology, University of Athens, Panepistimiopolis, Athens 157 01, Greece*

[2]*Department of Pharmacy, Laboratory of Pharmacology and Chemistry of Natural Products, University of Patras, 26500 Patras, Greece*

Received 12 July 2014; revised 11 September 2014; accepted 12 September 2014
Published online 17 September 2014 in Wiley Online Library (wileyonlinelibrary.com). DOI 10.1002/bip.22563

ABSTRACT:

Egg envelopes of vertebrates are composed of a family of proteins called zona pellucida (ZP) proteins, which are distinguished by the presence of a common structural polymerizing motif, known as ZP domain. Teleostean fish chorion is a fibrous structure, consisting of protein members of the ZPB/ZP1 and the ZPC/ZP3 families, which are incorporated as tandemly repeating heterodimers inside chorion fibers. Computational analysis of multiple ZPB/ZP1 proteins from several teleostean species, reveals two potential "aggregation-prone" sequence segments, forming a specific polymerization interface (AG interface). These two peptides were synthesized and results are presented in this work from transmission electron microscopy, Congo red staining, X-ray fiber diffraction and ATR FT-IR, which clearly display the ability of these peptides to self-aggregate, forming amyloid-like fibrils. This, most probably implies that the AG interface of ZPB/ZP1 proteins plays an important role for the formation of the repeating ZPB-ZPC heterodimers, which constitute teleostean chorion fibrils. © 2014 Wiley Periodicals, Inc. Biopolymers (Pept Sci) 102: 427–436, 2014.

Correspondence to: Stavros J. Hamodrakas, Department of Cell Biology and Biophysics, Faculty of Biology, University of Athens, Panepistimiopolis, Athens 157 01, Greece; e-mail: shamodr@biol.uoa.gr

Keywords: *functional protective amyloids; teleostean fish chorion;* zona pellucida *proteins; peptide-analogues; amyloid fibrils; vitelline envelope*

This article was originally published online as an accepted preprint. The "Published Online" date corresponds to the preprint version. You can request a copy of any preprints from the past two calendar years by emailing the Biopolymers editorial office at biopolymers@wiley.com.

INTRODUCTION

Eggs of all vertebrates are enclosed and protected by an acellular glycoproteinecous coat that is important for fertilization.[1,2] This coat is also implicated with prevention of polyspermy and protection of the embryo.[3–5] The nomenclature of this protective matrix, varies between different vertebrate groups, since it is known as chorion (or otherwise *zona radiata*) in teleostean fishes, *zona pellucida* in mammals and vitelline envelope in amphibians and birds.[6,7] Mammalian *zona pellucida*, is composed of three to four glycoproteins, early identified as ZP1/ZP4, ZP2, and ZP3, based on their molecular weights (200, 120, 82 kD respectively), which are expressed by the *ZPB*, *ZPA*, and *ZPC* gene subfamilies, respectively.[3,8–14] Conversely, teleostean fish chorion consists of a number of proteins that vary between species, and are expressed by the ZPB (ZP1-like) and ZPC (ZP3-like) gene subfamilies.[6,15–24] Besides the evident differences between vertebrate groups in number and function of egg envelope proteins, they all belong to a unique family of structural proteins, designated as ZP domain proteins.[25]

Teleostean fish ZP proteins, similar to mammalian, are incorporated into long interconnected filaments by forming

heterodimer building blocks,[3,9,10,26–29] after a post-translational C-terminal cleavage, crucial for secretion and polymerization.[25,28,30] They possess a structural polymerizing component, presenting high sequence homology, about 260 amino acids long, next to their C-terminal end. This module, known as a ZP domain, is distinguished by a conserved intramolecular disulfide bond pattern, extremely important for its structural integrity and function.[2,31] It is a bi-fold structure, which consists of two independently folded functional domains, termed ZP-N and ZP-C. There is evidence that the ZP-N domain is responsible for ZP protein polymerization.[28,32,33]

The egg envelope of *Austrofundulus limnaeus*, a teleostean fish, is composed of protein fibrils with amyloid characteristics.[34] Amyloids are insoluble fibrous protein aggregates, associated with pathological conditions.[35–38] However, their impressive functional architectures have been found to occasionally support important biological processes.[39–42] Recently, structural evidence revealed that the formation of human ZP protein dimers, may be mediated by a specific interface, found between the A and G β-strands (AG interface) of the ZP-N polymerization module of human ZP1.[43] In this respect, we sought to identify the possible amyloidogenic propensity of the A and G β-strands of the consensus sequence, representing the ZP-N domain of several characteristic teleostean ZPB proteins, derived by a multiple sequence alignment. Consequently, two corresponding peptide-analogues were sythesized, resembling the A and G β-strands of the consensus, based on the homology presented, compared to their hZP1 counterparts. Additionally, we utilized our consensus aggregation propensity prediction algorithm, "AMYLPRED2" freely accessible for academic use at http://biophysics.biol.uoa.gr/AMYLPRED2/[44,45] to test the "aggregation-prone" character of these two β-strands. Our experimental findings, demonstrate the formation of fibrils with distinct amyloidogenic properties, by self-aggregation of both peptides, possibly implicating, therefore, the AG interface in the ZP-N polymerization proccess of the teleostean ZPB chorion proteins.

Briefly, our experimental data clearly indicate that the AG interface of ZPB proteins is a highly self-"aggregation-prone" region. The aggregating potential of this specific segment might thus be the driving force behind the formation of the heterodimer building blocks composing teleostean ZP filaments and, therefore, may significantly contibute, similarly to human, to the formation of the ZP matrix of teleostean oocytes.

METHODS

Sequence Alignment

Amino acid sequences of ZPB (ZP1-like) proteins of several teleostean fish species were extracted from UniProt,[46] with the following accession numbers : P79817 (Japanese medaka); Q9W646 (Japanese medaka); Q91236 (Winter flounder); Q9I9M8 (Rainbow trout); Q9I9M7 (Rainbow trout); Q90356 (Common carp); Q90311 (Goldfish); Q9PWC8 (Zebrafish). A multiple sequence alignment was performed using ClustalW,[47] and a consensus sequence for the ZP-N domain of teleostean fish ZPB proteins was derived from this alignment (Figure 1a).

Homology Modeling

A three dimensional model depicting the ZP-N domain of the consensus teleostean ZPB sequence was built, using as template the available crystal structure of mouse ZP3 ZP-N domain (PDB ID: 3D4C),[49] applying comparative modelling techniques performed by MODELLER 9v2 (Figure 2).[50–52]

Prediction of Potential "Aggregation-prone" Segments and Peptide Synthesis

Two potential "aggregation-prone" peptides representing the A and G β-strands of the teleostean ZP-N domain consensus, VTVQCT and FELLFQC, were synthesized based on the homology to their hZP1 equivalents, with a simple substitution of the Cysteine (C) residue by Alanine (A), to avoid formation of undesired disulfide bonds, at neutral pH (peptides 1-6 and 95-101 of consensus, as seen in Figures 1b and 2b). Our AMYLPRED2 algorithm,[45] a consensus "aggregation-prone" protein segment predictor, was also utilized, to test the putative "aggregation-prone" character of these two peptides. The resulting peptides were designated as ZPF_A (VTVQAT) and ZPF_G (FELLFQA) respectively. Synthesis of the former was conducted by GeneCust Europe, Luxembourg (purity >98%, free N- and C-terminals), whereas for ZPF_G it was performed at the Laboratory of Pharmacognosy & Chemistry of Natural Products, Department of Pharmacy, University of Patras, Greece, utilizing similar methods to those reported previously.[53]

Formation of Amyloid-like Fibrils

Peptide solutions, in distilled water (pH 5.5), were prepared at two concentrations (5 and 15 mg ml^{-1}) for both peptides ZPF_A (VTVQAT) and ZPF_G (FELLFQA), and were found to spontaneously produce fibril-containing gels after 1- to 2-weeks incubation. The fibrils were judged to be mature, observing preparations both for shorter and longer periods than 1–2 weeks.

Transmission Electron Microscopy (Negative Staining)

For negative staining, fibril suspensions derived from the peptide solutions (at concentrations of 5 and 15 mg ml^{-1}), after incubation for 1–2 weeks, were applied to glow-discharged 400-mesh carbon-coated copper grids for 60 s. The grids were stained with a drop of 1% (w/v) aqueous uranyl acetate for 45 s. Excess stain was removed by blotting with a filter paper and the grids were air-dried. The grids were examined in a Philips CM10 electron microscope operated at 100 kV. Photographs were obtained by a retractable slow scan CCD camera (Gatan) utilizing the Digital Micrograph Software package (Gatan).

X-ray Diffraction

A droplet (10 μl) of fibril suspensions from the peptide solutions (15 mg ml^{-1}) from both peptides, after 1- to 2-weeks incubation, was

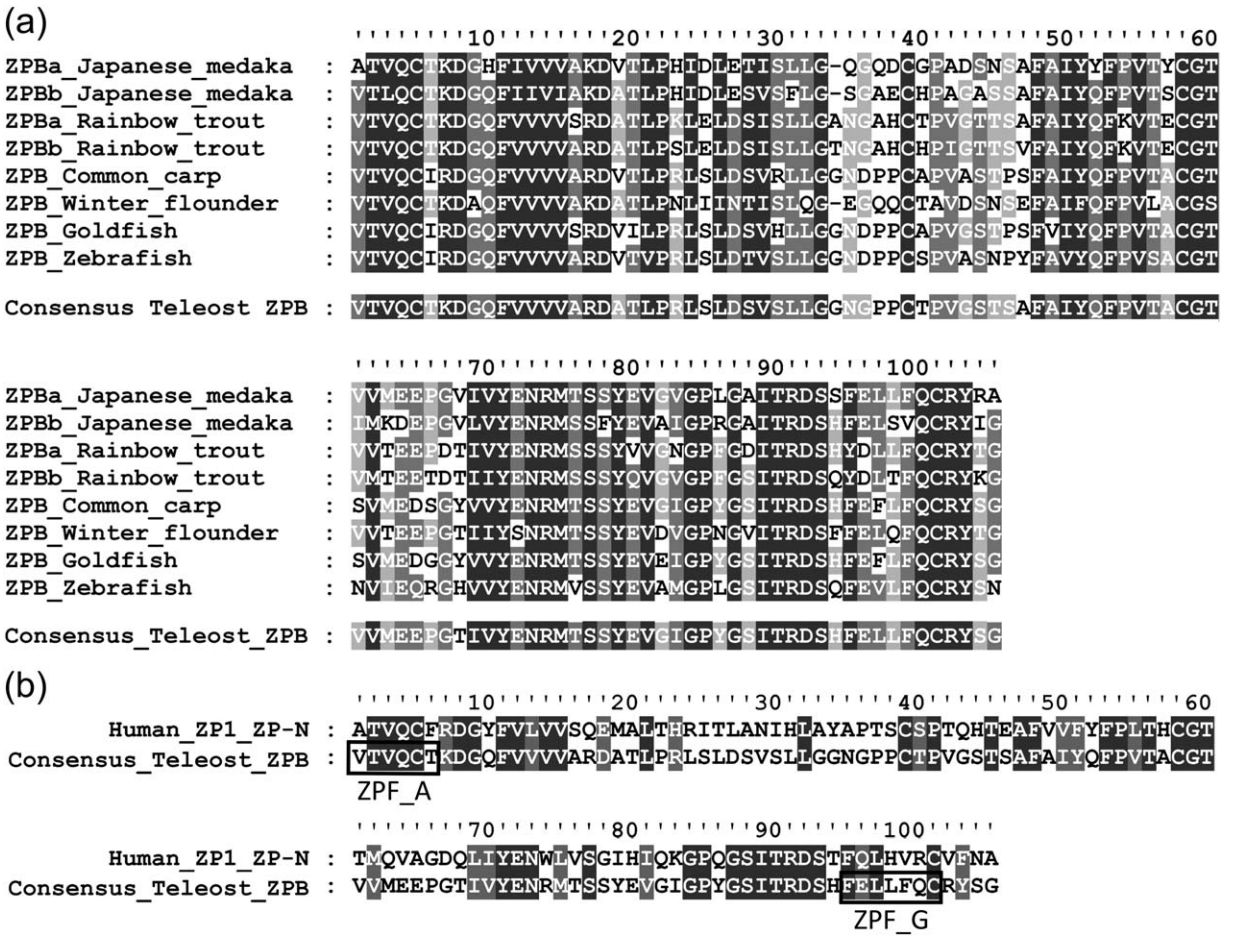

FIGURE 1 (a) Multiple sequence alignment of the teleostean ZPB ZP-N domain and generation of the derived consensus sequence. Sequences were aligned with ClustalW[47] and shading was perfomed by GeneDock.[48] (b) Sequence alignment of the teleostean ZPB ZP-N consensus to the human ZP1 ZP-N domain. Both synthesized peptide analogues ZPF_A and ZPF_G (corresponding to positions 1–6 and 95–101 of the consensus sequence, respectively) are enclosed in boxes and labelled. Black-boxed residues are identical, whereas grey-shaded residues represent 60 and 80% homology, respectively, from lighter to darker.

placed between two siliconized glass rods, spaced approximately 2 mm apart and mounted horizontally on a glass substrate. The droplet was allowed to dry slowly at ambient temperature and humidity for 30 min to form an oriented fiber, suitable for X-ray diffraction. X-ray fiber diffraction patterns were recorded on a Mar Research 345 mm image plate, utilizing Cu Kα radiation ($\lambda = 1.5418$ Å), obtained from a rotating anode generator (Rigaku MicroMax-007 HF—Osmic Rigaku VariMax^{TM} HF optics), operated at 40 kV, 20 mA. The specimen-to-film distance was set at 150 mm and the exposure time was 30 min. No additional low angle reflections were observed at longer specimen-to-film distances. The X-ray patterns, initially viewed using the program MarView (MAR Research, Hamburg, Germany), were displayed and measured with the aid of the program IPDISP of the CCP4 package.[54]

Congo Red Staining and Polarized Light Microscopy

A droplet of fibril suspensions derived from solutions of both peptides at a concentration of 5 mg ml^{-1}, was applied to glass slides and left to air-dry to form a thin film. Next, the film was stained with a 1% Congo red solution in distilled water (pH 5.75), at room temperature for approximately 20 minutes, according to the standard Románi protocol.[55] Finally, the samples were observed under bright field illumination and between crossed polars, using a Leica MZ75 polarizing stereomicroscope equipped with a JVC GC-X3E camera.

Attenuated Total Reflectance Fourier-transform Infrared (ATR FT-IR) Spectroscopy and Post-run Spectra Computations

Drops (5 μl) of the fibril suspensions, derived from the peptide solutions at 5 mg ml^{-1}, were cast on flat stainless-steel plates, coated with an ultrathin hydrophobic layer (SpectRIM, Tienta Sciences, IN) and were left to air-dry slowly at ambient conditions, to form thin hydrated films. IR spectra were obtained at a resolution of 4 cm^{-1}, utilizing an IR microscope (IRScope II, BrukerOPTICS, Bruker Optik GmbH, Ettlingen, Germany), equipped with a Ge ATR objective lens

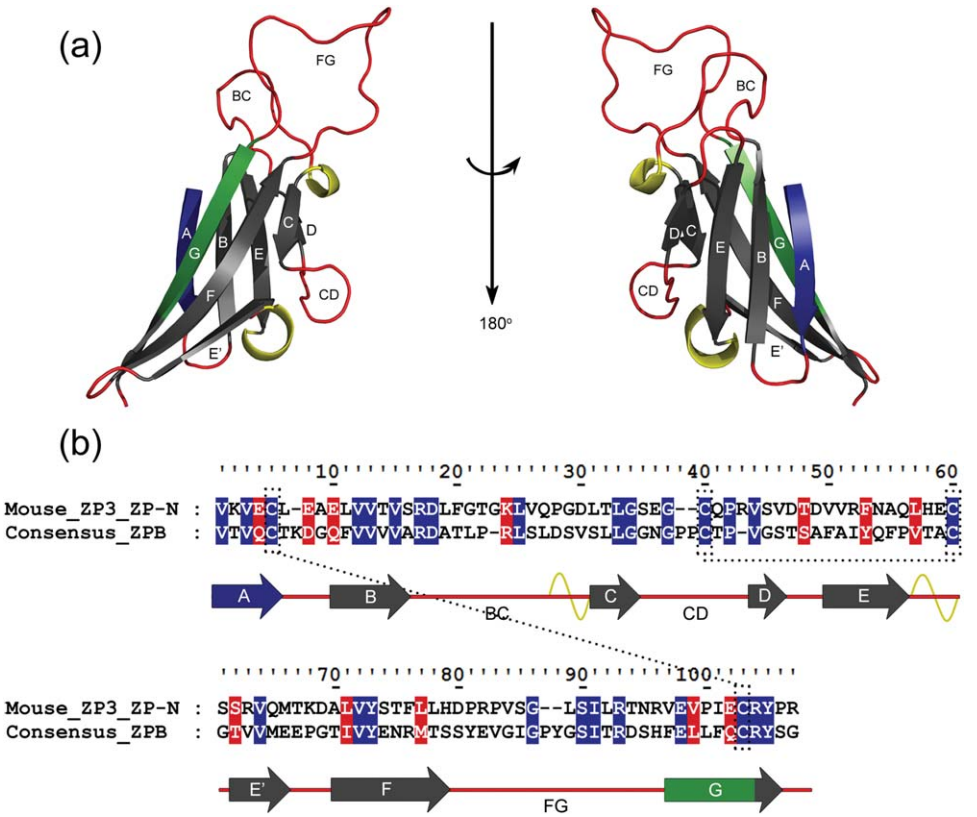

FIGURE 2 A structural model of the teleostean ZPB ZP-N consensus sequence, derived by homology modeling (see Methods). (a) Cartoon representation of the derived model, where β-strands are colored grey, α-helices yellow and loops red. The location of the ZPF_A peptide (A β-strand) is marked with blue, whereas the ZPF_G peptide (G β-strand) is shown in green. (b) Sequence alignment of the derived consensus to the sequence of the crystallographically determined ZP-N domain of mouse ZP3 (PDB ID: 3D4C). Blue-boxed residues are identical, whereas red-boxed represent at least 60% homology, respectively. A representation of the secondary structural elements is also shown (arrows represent β-strands, coils represent α-helices), in addition to the conserved disulfide bond pattern formed (dotted lines).

(20×) and attached to a FT spectrometer (Equinox 55, BrukerOPTICS). Ten 32-scan spectra were collected from each sample and averaged to improve the Sound/Noise (S/N) ratio. All spectra are shown in the absorption mode after correction for the wavelength-dependence of the penetration depth (d_p analogous to λ). Absorption band maxima were determined from the minima in the second derivative of the corresponding spectra. Derivatives were computed analytically using routines of the OPUS/OS2 software after a 13 point smoothing around each data point, by the Savitsky–Golay algorithm.[56] Smoothing over narrower ranges resulted in deterioration of the *S/N* ratio and did not increase the number of minima that could be determined with confidence.

Docking Experiments

The modeled structure of the consensus ZPB ZP-N domain was used to perform docking experiments, in order to confirm the role of the AG interface, formed by the ZPF_A and ZPF_G "aggregation-prone" peptides, as a potential interface for ZP-N dimer formation. To obtain a structural model of a ZPB ZP-N homodimer, the HADDOCK version 2.1 was used.[57] Interaction restraints to drive the docking were defined unambiguously (are not subjected to random removal). Pairs of C_a interatomic distances of 5 ± 1 Å were set concerning residues 1–6 and 95–101 of the modeled structure (concering the ZPF_A and ZPF_G peptide locations, respectively) in order to investigate the possibility of a ZPB ZP-N homodimer with self-interacting A and G β-strands in an antiparallel fashion (a parallel spatial arrangement is not possible). Structure calculations were performed by CNS1.2,[58] whereas non-bonded interactions were calculated with the OPLS force field[59] using an 8.5 Å cutoff. The solvated docking protocol[60] was preferred, since in comparison to unsolvated docking it may yield higher quality docking predictions.[61]

RESULTS

Both "aggregation-prone" ZPF_A and ZPF_G peptides self-assemble into fibrils, after solution in distilled water (at varying concentrations) and incubation for 1–2 weeks. Negative staining reveals that ZPF_A fibrils have the structural characteristics

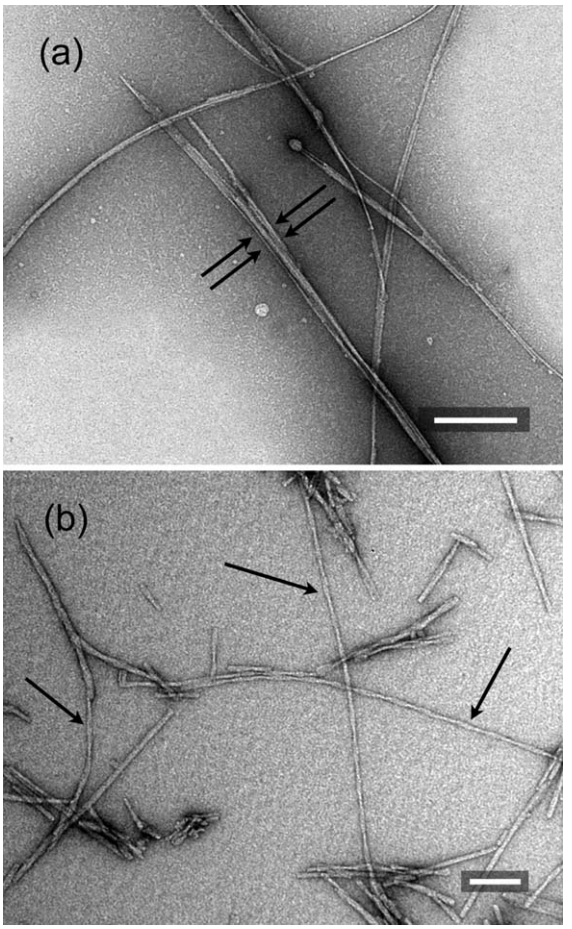

FIGURE 3 Electron micrographs of fibrils derived by self-assembly of the "aggregation-prone" peptides. (a) Fibrils formed by the ZPF_A peptide appear as long, straight and unbranched filaments. Additionally, they tend to interact laterally forming local aggregates (marked with double arrows) and occasionally ribbons. Bar 500 nm. (b) Filaments formed by the ZPF_G peptide are also viewed as straight and unconnected filaments of various lengths. Moreover, they occasionally tend to coalesce forming double helical structures of 100–120 Å in width (single arrows). Bar: 100 nm.

of amyloid-like fibrils. Specifically, they appear as long fibrils of indeterminate length, with a width of ~100–120 Å, which interact in a lateral fashion (Figure 3a). Equivalently, fibrils formed by the ZPF_G peptide resemble amyloid-like fibrils, since they are straight and unbranched double helices of indeterminate length, with a diameter of ~100–120 Å. Each double-helical filament consists of two protofilaments, with a uniform diameter of ~50–70 Å, which wound around each other (Figure 3b).

Amyloids have been found to specifically bind the Congo red dye.[62,63] Hence, gels of fibrils derived by the ZPF_A and ZPF_G peptides were stained with Congo red and examined under a polarizing microscope. It is clear, in both cases, that amyloid deposits formed by these two peptides, bind Congo red (bright field illumination) and furthermore, exhibit a characteristic for amyloid fibrils apple/green birefringence, when viewed under crossed polars (Figure 4).

The X-ray diffraction pattern, produced by an oriented fiber containing ZPF_A amyloid-like fibrils is a typical "cross-β" diffraction pattern observed for several amyloid-like fibrils,[63,64] in which the β-strands are perpendicular to the fiber axis and the β-sheets are packed parallel to the fiber axis (Figure 5a). The intense meridional reflection at 4.7 Å is due to the distance between hydrogen-bonded β-strands, aligned perpendicular to the main fiber axis, whereas the 9.1 Å reflection arises from the spacing between packed β-sheets that are oriented in a parallel fashion to the fibrillar axis (Table I). The additional 21.4 Å equatorial reflection observed, could be assigned to tandem repeats of the length of the ZPF_A hexapeptide (6 residues × 3.5–3.6 Å per residue ~21.4 Å), arising from the interaction of adjacent molecules. Similarly, a characteristic "cross-β" X-ray diffraction pattern is produced by a ZPF_G peptide oriented fiber (Figure 5b). The strong reflections corresponding to periodicities of 4.7 and 10.4 Å are attributed to the inter-strand and inter-sheet distances of β-sheet arrangements, respectively. The observed difference between equatorial reflections of the ZPF_A and ZPF_G peptides most likely indicates a difference in packing distance of the packed β-sheets. The ZPF_A hexapeptide is composed mostly of residues with short side chains whereas the ZPF_G peptide is composed of bulky residues. Moreover, a detailed search of ZipperDB,[67] revealed a structural crystallographic model for the ZPF_A peptide (VTVQAT), whereas a crystallographically determined model of a similar peptide (LELLFQ) to ZPF_G (FELLFQA) was also found. Detailed analysis of both structures, revealed that the packing distances between the β-sheets formed by adjacent peptides have an average distance of 9.1 and 10.7 Å, respectively in each model, in close agreement to what was observed in our X-ray data (9.1 and 10.4 Å, respectively). Reflections appear as rings due to the poor alignment of the oriented fiber constituent fibrils (Table I).

Important information, referring to the secondary structure of peptides forming amyloid fibrils was also obtained through ATR FT-IR spectral acquisitions. In both cases, the ATR FT-IR spectra derived from thin hydrated films from amyloid fibrils from both peptides, clearly indicate the preponderance of an antiparallel β-sheet secondary structure for the peptides forming the amyloid-like fibrils. In particular, the ATR FT-IR spectrum of the ZPF_A peptide fibrils (Figure 6a) contains a dominant 1630 cm^{-1} Amide I band, supported by the 1531 cm^{-1} Amide II and 1231 cm^{-1} Amide III bands, all indicative of a β-sheet secondary structure.[68–70] Similarly, the ZPF_G spectrum (Figure 6b) shows one prominent band at

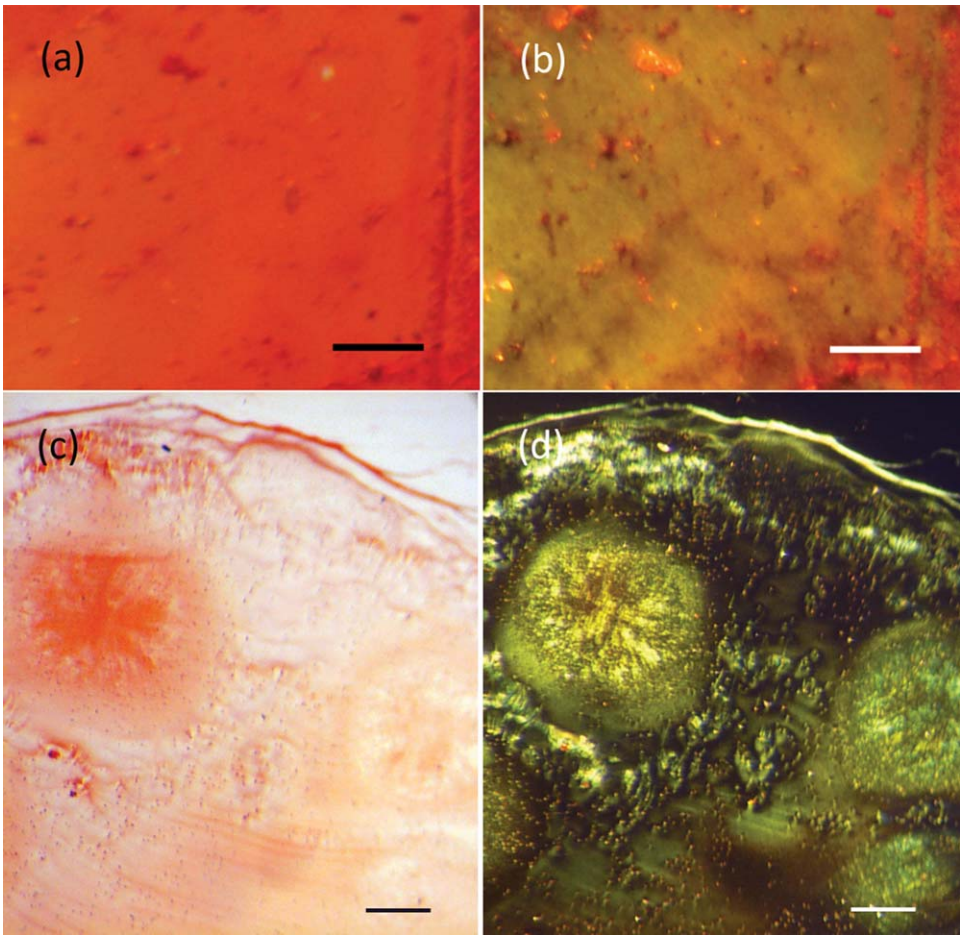

FIGURE 4 Photomicrographs of amyloid fibril-containing gels stained with Congo red (see Materials and Methods). Fibrils derived from ZPF_A (a, b) and ZPF_G (c, d) peptide analogue fibrils bind the Congo red dye, as seen under bright field illumination (a, c). The typical for amyloid fibrils apple-green birefringence is clearly seen, under crossed polars (b, d). Bar 300 μm.

1632 cm^{-1} in the Amide I region, indicative of β-sheet. Additionally, the amide III band at 1234 cm^{-1} supports our assumptions based on the amide I band. Finally, an additional component located at 1692 and 1691 cm^{-1}, in the ZPF_A and ZPF_G spectra respectively, is a strong indication that the β-sheets are ordered in an antiparallel fashion, since proteins containing antiparallel β-sheets frequently present a β-sheet component arising from transition dipole coupling usually 50–70 cm^{-1} higher than the prominent β-sheet band.[69] Thus, all ATR FT-IR evidence supports the presence of uniform antiparallel β-sheets as the dominant secondary structure for both peptides (Table II), in agreement with the evidence obtained by the characteristic X-ray "cross-β" patterns.

DISCUSSION

Clearly, our experimental results indicate that both ZPF_A and ZPF_G peptides "self-aggregate," forming fibrils, which exhibit all the basic characteristics of amyloid fibrils, as mentioned above.

Detailed studies have previously highlighted the ZP-N domain as responsible for ZP protein polymerization.[28,32,33,71] In particular, recent evidence, suggests that ZP3-ZP2 and ZP3-ZP1 heterodimers composing mammalian ZP filaments, may be formed by the aggregation propensity of a specific surface region of their ZP-N domains, called AG interface, shaped by the, adjacent in space, A and G β-strands.[43] For this purpose, a model of the ZP-N domain structure of the teleostean consensus sequence was created, based on its high homology to the sequence of the crystallographically solved structure of the ZP-N domain of mouse ZP3 protein.[49] As seen by the derived model, ZP-N domains of ZPB proteins of teleostean fish, most probably, adopt an Ig-like antiparallel β-sandwich fold, stabilized by the presence of two disulfide bonds formed between their invariant Cys residues, with two antiparallel β-sheets, each composed of four β-strands (A to G), similar to the

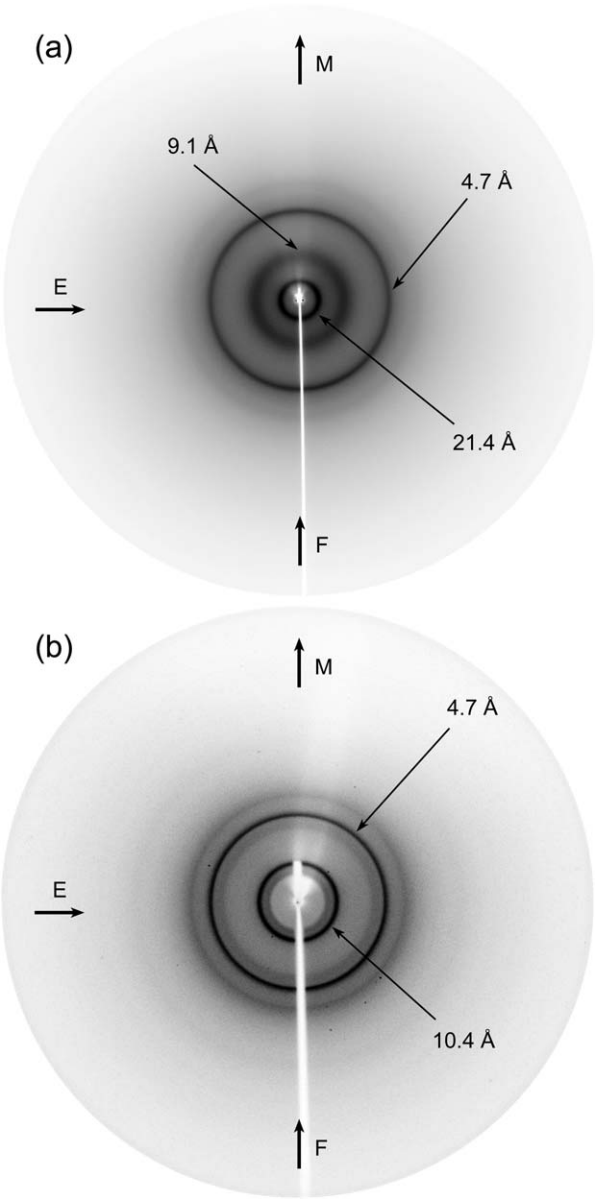

FIGURE 5 X-ray diffraction patterns produced from oriented fibers of mature fibril suspensions produced by the ZPF_A and ZPF_G peptides. The meridian, M (direction parallel to the fiber axis, F) is vertical and the equator, E, is horizontal in this display. (a) The X-ray diffraction pattern produced by the ZPF_A peptide clearly resembles a "cross-β" pattern,[64–66] with an intense meridional 4.7 Å reflection, corresponding to the spacing of successive hydrogen bonded β-strands aligned perpendicular to the fiber axis and a 9.1 Å reflection, on the equator, attributed to the packing distance of β-sheets (Table I). (b) Similarly, a "cross-β" diffraction pattern is produced by the ZPF_G peptide, since the 4.7 and 10.4 Å reflections are indicative of the inter-strand and inter-sheet distances, respectively (Table I). Because of poor alignment of fibrils reflections appear as rings.

mammalian ZP protein ZP-N domains (Figure 2).[33,49,71] Accordingly, the "aggregation-prone" ZPF_A and ZPF_G peptide regions were located within the AG interface of the modelled structure, as expected. Subsequently, docking experiments (see Materials and Methods), clearly demonstrate that ZPB ZP-N dimers of the modeled structure can be formed through interacting AG interfaces (Figure 7). The optimal solution had a HADDOCK score of −60.4 (Van der Waals energy of −32.3, electrostatic energy of −202.8, desolvation energy of +12.5 kcal mol^{-1} and no restraints violation energy, respectively) with a total buried surface area of 1463.1 $Å^2$.

Table I Spacings of the Reflections Observed in the X-ray Diffraction Patterns Obtained from Oriented Fibers, Containing Amyloid Fibrils, Derived by ZPF_A and ZPF_G Self-assembly

			d_{obs} (Å)	
h	*k*	*l*	ZPF_A	ZPF_G
1	0	0	4.7	4.7
0	1	0	9.1	10.4
0	0	1	21.4	

Previous studies have indicated that the edge β-strands of proteins possessing an Ig-like fold, play a vital role in the formation of dimers and higher order homopolymers.[72] Strategically placed β-bulges, charged or proline residues and covering secondary structure elements protect soluble monomers from polymerizing, via edged aggregation-prone β-strands.[72] In contrast, proteins that natively form hydrogen bonded homodimers, such as tranthyretin[73] or human ZP proteins[43] usually possess edged β-strands with long regular stretches that present none of the aforementioned protective features, similarly to the ZPF_A and ZPF_G peptides. Furthermore, recent impressive experiments indicate that isolated interface stretches of homopolymer-forming proteins, possess a self-assembly propensity preserving in that manner properties of their parental interfaces.[74] Equivalently, both ZPF_A and ZPF_G isolated

Table II Bands Observed in the ATR FT-IR Spectrum of a Hydrated Film Produced from a Suspension of Fibrils, Produced by the ZPF_A Peptide and ZPF_G Peptide, Respectively, and their Tentative Assignments

Bands (cm^{-1})		
ZPF_A	ZPF_G	Assignments
1137	1140	TFA
1182	1184	TFA
1202	1200	TFA
1231	1234	β-sheet (Amide III)
	1515	Phe
1531	1550	β-sheet (Amide II)
1630	1632	β-sheet (Amide I)
1666	1668	TFA
1692	1691	Antiparallel β-sheet (Amide I)

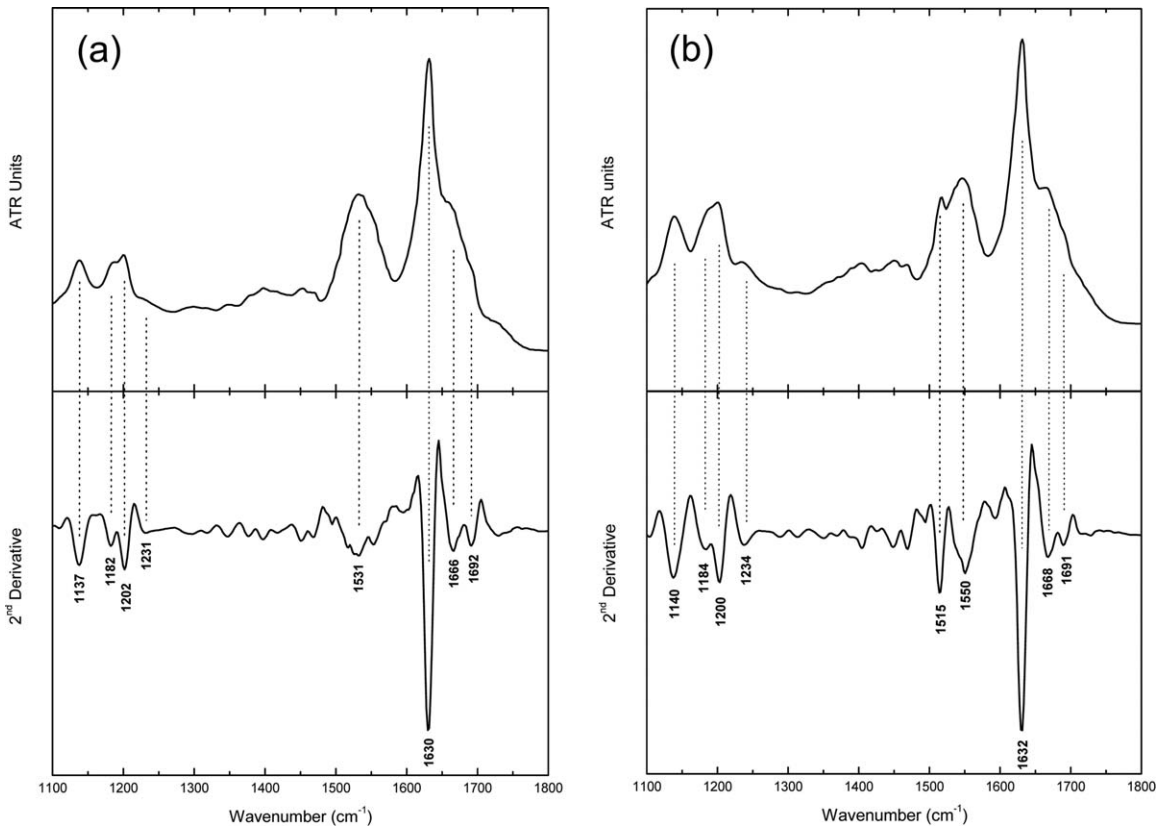

FIGURE 6 ATR FT-IR (1100–1800 cm^{-1}) spectra obtained from thin hydrated-films containing mature amyloid-like fibrils from the (a) ZPF_A and (b) ZPF_G peptides. Second derivative spectra are also included and were used for the exact identification of the band maxima and their tentative assignments. The resulting spectra, in both cases, clearly indicate an antiparallel β-sheet conformation as the dominant secondary structure of fibrils formed by each aggregation-prone peptide (Table II).

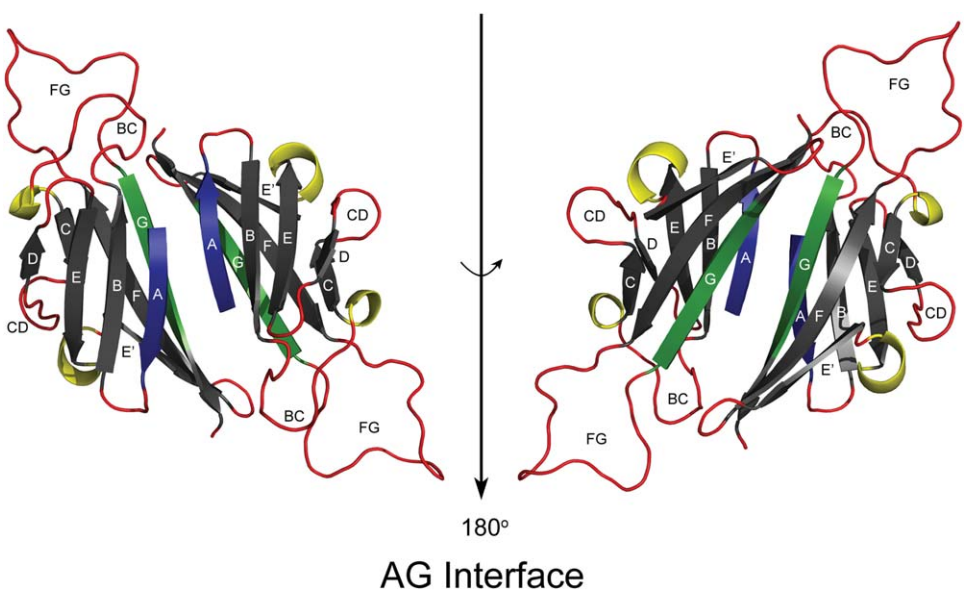

FIGURE 7 The formation of ZPB ZP-N dimers, through their interacting AG interfaces (formed by the ZPF_A and ZPF_G aggregation-prone peptides). Docking procedures, performed by the HADDOCK algorithm, provided this structural model (see Materials and Methods). In the cartoon representation, β-sheets are colored grey, helices are yellow and loops with red. The location of both ZPF_A and ZPF_G aggregation-prone peptides is shown in the structure, since the former is shown in blue and the latter with green.

peptides exhibit "aggregation-prone" properties, possibly retaining the self-aggregation potential of the parental properties of the AG interface of ZPB teleostean proteins.

Namely, our experimental data, which clearly show that both ZPF_A and ZPF_G peptide segments are "self-aggregating" peptides, together with the docking attempts, indicate that the AG interface of the ZP-N domain is most probably responsible for the polymerization of the teleostean fish ZP proteins (Figure 7), in a way similar to the human ZP-N domains.[43]

CONCLUSIONS

Our experimental observations indicate that this moderately conserved "aggregation-prone" surface segment of the ZP-N domain of ZPB proteins retains the self-aggregating potential to drive ZPB proteins into dimers and therefore, subsequently, to allow them to polymerize forming filaments.

Aside from previous experimental data, exposing the ability of chorion proteins of the *Austrofundulus limnaeus* teleostean fish, to form amyloid-like fibrils that bind the characteristic Congo red dye,[34] it is our belief that the data presented here suggest that teleostean fish chorion is an important functional amyloid, protecting fish oocytes, similarly to silkmoth chorion and human *zona pellucida*.[41,43,75,76] We consider future studies to be crucial, in order to further validate our results, by identifying similar "aggregation-prone" surfaces of ZPC proteins, also found present in teleostean chorion, as well as the possible contribution of the ZP-C domain in teleostean fish chorion protein polymerization. The aftereffects of identifying novel natural amyloids might have a significant impact in biomaterials development, by exploiting the impressive mechanical and structural properties that these structures possess.[77–81]

The authors thank Peter Everitt of EMBL, Heidelberg for excellent technical assistance and continuous unfailing help. They sincerely thank the editor for properly handling this manuscript and the anonymous reviewers for their very useful and constructive criticism, which helped them to improve considerably the manuscript. They also thank the University of Athens for support.

REFERENCES

1. Dumont, J. N.; Brummett, A. R. Dev Biol (New York) 1985, 1, 235–288.
2. Monné, M.; Han, L.; Jovine, L. Semin Reprod Med 2006, 24, 204–216.
3. Wassarman, P. M. Annu Rev Biochem 1988, 57, 415–442.
4. Brivio, M. F.; Bassi, R.; Cotelli, F. Mol Reprod Dev 1991, 28, 85–93.
5. Hyllner, S. J.; Westerlund, L.; Olsson, P. E.; Schopen, A. Biol Reprod 2001, 64, 805–811.
6. Spargo, S. C.; Hope, R. M. Biol Reprod 2003, 68, 358–362.
7. Conner, S. J.; Lefievre, L.; Hughes, D. C.; Barratt, C. L. Hum Reprod 2005, 20, 1148–1152.
8. Repin, V. S.; Akimova, I. M. Biokhimiia 1976, 41, 50–57.
9. Bleil, J. D.; Wassarman, P. M. Dev Biol 1980, 76, 185–202.
10. Greve, J. M.; Wassarman, P. M. J Mol Biol 1985, 181, 253–264.
11. Wassarman, P. M. Sci Am 1988, 259, 78–84.
12. Boja, E. S.; Hoodbhoy, T.; Fales, H. M.; Dean, J. J Biol Chem 2003, 278, 34189–34202.
13. Boja, E. S.; Hoodbhoy, T.; Garfield, M.; Fales, H. M. Biochemistry 2005, 44, 16445–16460.
14. Gupta, S. K.; Bhandari, B.; Shrestha, A.; Biswal, B. K.; Palaniappan, C.; Malhotra, S. S.; Gupta, N. Cell Tissue Res 2012, 349, 665–678.
15. Oppen-Berntsen, D. O.; Helvik, J. V.; Walther, B. T. Dev Biol 1990, 137, 258–265.
16. Hyllner, S. J.; Oppen-Berntsen, D. O.; Helvik, J. V.; Walther, B. T.; Haux, C. J Endocrinol 1991, 131, 229–236.
17. Oppen-Berntsen, D. O.; Hyllner, S. J.; Haux, C.; Helvik, J. V.; Walther, B. T. Int J Dev Biol 1992, 36, 247–254.
18. Lyons, C. E.; Payette, K. L.; Price, J. L.; Huang, R. C. J Biol Chem 1993, 268, 21351–21358.
19. Murata, K.; Sasaki, T.; Yasumasu, S.; Iuchi, I.; Enami, J.; Yasumasu, I.; Yamagami, K. Dev Biol 1995, 167, 9–17.
20. Chang, Y. S.; Wang, S. C.; Tsao, C. C.; Huang, F. L. Mol Reprod Dev 1996, 44, 295–304.
21. Murata, K.; Sugiyama, H.; Yasumasu, S.; Iuchi, I.; Yasumasu, I.; Yamagami, K. Proc Natl Acad Sci USA 1997, 94, 2050–2055.
22. Sugiyama, H.; Yasumasu, S.; Murata, K.; Iuchi, I.; Yamagami, K. Dev Growth Differ 1998, 40, 35–45.
23. Oppen-Berntsen, D. O.; Arukwe, A.; Yadetie, F.; Lorens, J. B.; Male, R. Mar Biotechnol (N Y) 1999, 1, 252–260.
24. Conner, S. J.; Hughes, D. C. Reproduction 2003, 126, 347–352.
25. Jovine, L.; Darie, C. C.; Litscher, E. S.; Wassarman, P. M. Annu Rev Biochem 2005, 74, 83–114.
26. Grierson, J. P.; Neville, A. C. Tissue Cell 1981, 13, 819–830.
27. Wassarman, P. M.; Mortillo, S. Int Rev Cytol 1991, 130, 85–110.
28. Jovine, L.; Qi, H.; Williams, Z.; Litscher, E. S.; Wassarman, P. M. Proc Natl Acad Sci USA 2004, 101, 5922–5927.
29. Litscher, E. S.; Wassarman, P. M. Histol Histopathol 2007, 22, 337–347.
30. Jimenez-Movilla, M.; Dean, J. J Cell Sci 2011, 124, 940–950.
31. Bork, P.; Sander, C. FEBS Lett 1992, 300, 237–240.
32. Jovine, L.; Janssen, W. G.; Litscher, E. S.; Wassarman, P. M. BMC Biochem 2006, 7, 11.
33. Han, L.; Monne, M.; Okumura, H.; Schwend, T.; Cherry, A. L.; Flot, D.; Matsuda, T.; Jovine, L. Cell 2010, 143, 404–415.
34. Podrabsky, J. E.; Carpenter, J. F.; Hand, S. C. Am J Physiol Regul Integr Comp Physiol 2001, 280, R123–R131.
35. Dobson, C. M. Trends Biochem Sci 1999, 24, 329–332.
36. Dobson, C. M. Nature 2003, 426, 884–890.
37. Chiti, F.; Dobson, C. M. Annu Rev Biochem 2006, 75, 333–366.
38. Fandrich, M. Cell Mol Life Sci 2007, 64, 2066–2078.
39. Kelly, J. W.; Balch, W. E. J Cell Biol 2003, 161, 461–462.
40. Fowler, D. M.; Koulov, A. V.; Balch, W. E.; Kelly, J. W. Trends Biochem Sci 2007, 32, 217–224.
41. Iconomidou, V. A.; Hamodrakas, S. J. Curr Protein Pept Sci 2008, 9, 291–309.

42. Maury, C. P. J Intern Med 2009, 265, 329–334.
43. Louros, N. N.; Iconomidou, V. A.; Giannelou, P.; Hamodrakas, S. J. PLoS One 2013, 8, e73258.
44. Frousios, K. K.; Iconomidou, V. A.; Karletidi, C. M.; Hamodrakas, S. J. BMC Struct Biol 2009, 9, 44.
45. Tsolis, A. C.; Papandreou, N. C.; Iconomidou, V. A.; Hamodrakas, S. J. PLoS One 2013, 8, e54175.
46. Consortium, T. U. Nucleic Acids Res 2009, 37, D169–D174.
47. Thompson, J. D.; Higgins, D. G.; Gibson, T. J. Nucleic Acids Res 1994, 22, 4673–4680.
48. Nicholas, K. B.; Nicholas, H. B. J.; Deerfield, D. W. EMBNEW-NEWS 1997, 4, 14.
49. Monné, M.; Han, L.; Schwend, T.; Burendahl, S.; Jovine, L. Nature 2008, 456, 653–657.
50. Sali, A.; Blundell, T. L. J Mol Biol 1993, 234, 779–815.
51. Eswar, N.; John, B.; Mirkovic, N.; Fiser, A.; Ilyin, V. A.; Pieper, U.; Stuart, A. C.; Marti-Renom, M. A.; Madhusudhan, M. S.; Yerkovich, B.; Sali, A. Nucleic Acids Res 2003, 31, 3375–3380.
52. Eswar, N.; Webb, B.; Marti-Renom, M. A.; Madhusudhan, M. S.; Eramian, D.; Shen, M. Y.; Pieper, U.; Sali, A. Curr Protoc Bioinform 2006, 5, Unit 5 6.
53. Iconomidou, V. A.; Cordopatis, P.; Hoenger, A.; Hamodrakas, S. J. Biopolymers 2011, 96, 723–733.
54. Bailey, S. Acta Crystallogr Sect D Biol Crystallogr 1994, 50, 760–763.
55. Romhanyi, G. Virch Arch A Pathol Pathol Anat 1971, 354, 209–222.
56. Savitsky, A.; Golay, M. J. E. Anal Chem 1967, 36, 1627–1639.
57. de Vries, S. J.; van Dijk, A. D.; Krzeminski, M.; van Dijk, M.; Thureau, A.; Hsu, V.; Wassenaar, T.; Bonvin, A. M. Proteins 2007, 69, 726–733.
58. Brunger, A. T.; Adams, P. D.; Clore, G. M.; DeLano, W. L.; Gros, P.; Grosse-Kunstleve, R. W.; Jiang, J. S.; Kuszewski, J.; Nilges, M.; Pannu, N. S.; Read, R. J.; Rice, L. M.; Simonson, T.; Warren, G. L. Acta Crystallogr D Biol Crystallogr 1998, 54, 905–921.
59. Jorgensen, W. L.; Tirado-Rives, J. J Am Chem Soc 1988, 110, 1657–1666.
60. van Dijk, A. D.; Bonvin, A. M. Bioinformatics 2006, 22, 2340–2347.
61. Kastritis, P. L.; Visscher, K. M.; van Dijk, A. D.; Bonvin, A. M. Proteins 2012, 81, 510–518.
62. Divry, D.; Florkin, M. Comptes Rendus Soc Biol 1927, 97, 1808–1810.
63. Sunde, M.; Blake, C. Adv Protein Chem 1997, 50, 123–159.
64. Geddes, A. J.; Parker, K. D.; Atkins, E. D.; Beighton, E. J Mol Biol 1968, 32, 343–358.
65. Fraser, R. D. B.; MacRae, T. P. Conformation in Fibrous Proteins and Related Synthetic Polypeptides; Academic Press: New York, 1973.
66. Jahn, T. R.; Makin, O. S.; Morris, K. L.; Marshall, K. E.; Tian, P.; Sikorski, P.; Serpell, L. C. J Mol Biol 2010, 395, 717–727.
67. Goldschmidt, L.; Teng, P. K.; Riek, R.; Eisenberg, D. Proc Natl Acad Sci USA 2010, 107, 3487–3492.
68. Krimm, S.; Bandekar, J. Adv Protein Chem 1986, 38, 181–364.
69. Surewicz, W. K.; Mantsch, H. H.; Chapman, D. Biochemistry 1993, 32, 389–394.
70. Jackson, M.; Mantsch, H. H. Crit Rev Biochem Mol Biol 1995, 30, 95–120.
71. Monne, M.; Jovine, L. Biol Reprod 2011, 85, 661–669.
72. Richardson, J. S.; Richardson, D. C. Proc Natl Acad Sci USA 2002, 99, 2754–2759.
73. Palaninathan, S. K.; Mohamedmohaideen, N. N.; Snee, W. C.; Kelly, J. W.; Sacchettini, J. C. J Mol Biol 2008, 382, 1157–1167.
74. Valery, C.; Pandey, R.; Gerrard, J. A. Chem Commun 2013, 49, 2825–2827.
75. Iconomidou, V. A.; Vriend, G.; Hamodrakas, S. J. FEBS Lett 2000, 479, 141–145.
76. Iconomidou, V. A.; Chryssikos, G. D.; Gionis, V.; Vriend, G.; Hoenger, A.; Hamodrakas, S. J. FEBS Lett 2001, 499, 268–273.
77. Mitraki, A. Adv Protein Chem Struct Biol 2010, 79, 89–125.
78. Cherny, I.; Gazit, E. Angew Chem Int Ed Engl 2008, 47, 4062–4069.
79. Gras, S. L.; Tickler, A. K.; Squires, A. M.; Devlin, G. L.; Horton, M. A.; Dobson, C. M.; MacPhee, C. E. Biomaterials 2008, 29, 1553–1562.
80. Mankar, S.; Anoop, A.; Sen, S.; Maji, S. K. Nano Rev 2011, 2.
81. Knowles, T. P.; Buehler, M. J. Nat Nanotechnol 2011, 6, 469–479.